Review, modeling, Heat Integration, and improved schemes of Rectisol®-based processes for CO_2 capture

Manuele Gatti [a,*], Emanuele Martelli [a], François Marechal [b], Stefano Consonni [a]

[a] Politecnico di Milano, Dipartimento di Energia, via Lambruschini 4, Milano 20156, Italy
[b] Industrial Process Energy Systems Engineering (IPESE), Ecole Polytechnique Fédérale de Lausanne, 1015 Lausanne, Switzerland

Received 5 January 2014
Received in revised form
24 April 2014
Accepted 1 May 2014
Available online 10 May 2014

1. Introduction

Coal to Liquids (CTL) as well as Coal to Substitute Natural Gas (Coal-to-SNG) and Integrated Gasification Combined Cycle (IGCC) plants can exploit and convert cheap fossil fuels, like coal, petcoke, waste and biomass, into a clean synthetic gas, mainly composed of hydrogen, carbon monoxide, carbon dioxide and other minor species, to produce either liquid fuels or electricity. Within this syngas conversion process, a key step is the removal of sulphur species (i.e., H_2S, COS, CS_2, mercaptans and organic sulfides) which poison downstream catalysts and, if syngas is burned in a gas turbine or boiler, originate SO_2. For this reason, coal gasification plants always include an Acid Gas Removal (AGR) unit capable of abating the content of sulphur species in syngas below the limits imposed by the downstream processes, e.g. 50 ppb for a Fischer–Tropsch (FT) synthesis catalysts and 50 ppm for gas turbines. Besides H_2S removal, AGR units are also suitable to separate CO_2 from syngas and make it available as an almost pure separate stream, ready for utilization or long-term sequestration. This feature has been exploited so far only in those gasification-based polygeneration plants co-producing urea or other chemicals requiring CO_2 as a feedstock [1], and in the North Dakota coal gasification facility [2]to make available a CO_2 stream for Enhanced Oil Recovery (EOR) (see e.g., [3]). However, this capability of selectively removing H_2S and CO_2 will become even more attractive in case of a future implementation of Carbon Capture and Storage (CCS). Indeed, according

* Corresponding author. Tel.: +39 0523 35 6872.
E-mail address: manuele.gatti@polimi.it (M. Gatti).

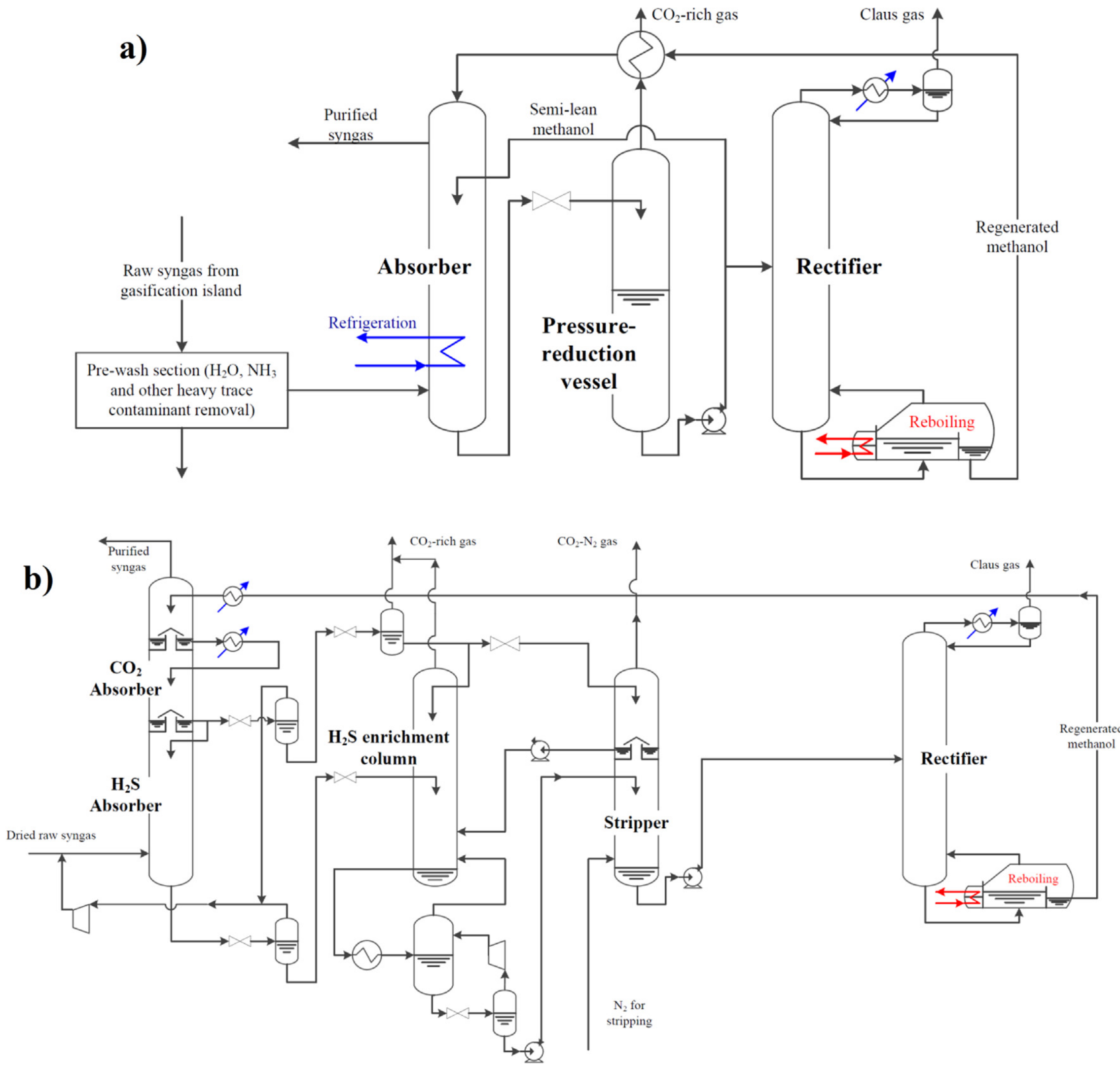

Fig. 1. a) Lurgi (adapted from Ref. [11]) and b) Linde [12] patented Rectisol®.

to a mid-term perspective, in an electricity market characterized by restrictions on CO_2 emissions, CCS is likely to become a key feature of IGCC power plants [4].

For similar reasons, as far as the production of "low-carbon emissions" liquid fuels is concerned, the conversion of coal into synthetic liquids with CCS (capturing the carbon in excess to the synthetic fuel content) seems to be one of the most promising and viable options to provide an alternative to oil derived fuels, capable of being competitive in terms of economics, environmental impact and energy security, especially when high oil prices are envisaged [5]. Recently different authors have investigated the feasibility and attractiveness of co-gasification with biomass to further reduce the carbon footprint (see for instance the study of Kreutz et al. [6] and the extensive review by Floudas et al. [7]).

In addition, the large number of gasification-based facilities available worldwide which, as reported by Higman [8], amounts to 618 operating gasifiers and 234 projects (for a total syngas capacity of 104.7 GWth) makes pre-combustion CO_2 capture via AGR processes one of the most well-proven and promptly avail-able CCS strategies. Indeed, twelve out of the "active" planned gasification-based projects listed by the gasification database [9] are going to feature an AGR specifically tailored for CO_2 separation.

On the other hand, if CO_2 separation and CCS are implemented, the energy consumption of the AGR unit considerably grows becoming the second highest energy consumption among the auxiliaries of the overall plant (the first one is the Air Separation Unit), as shown in [10]. For instance, according to [10], when implementing CCS in an IGCC featuring a Shell gasifier, the electric power consumption and the capital cost of the Selexol® AGR pro-cess (including the CO_2 compressor) increase from 1.0 MW and 47.7 M€ (design tailored for the removal of H_2S) to 54.9 MW and 217.7 M€ (i.e., 3 percentage points of LHV efficiency). Since the AGR process has such considerable impact on the thermodynamic and economic performance of the plant, it is very useful at the design stage to have (1) a detailed process model that can accurately predict the separation effectiveness, (2) an approach to evaluate the possible Heat Integration opportunities without neglecting the interactions with the rest of the plant.

In this paper, we focus on the Rectisol® process, a methanol-based physical absorption process patented and developed by Lurgi [11] and Linde [12] and widely used for the selective removal of H_2S and CO_2 from coal-derived syngas [13]. Its first installation was built during the 1950s by Lurgi at the Sasol-Secunda CTL plant in South Africa, in the form of three identical scrubbing trains releasing an acid gas stream, consisting of 98.5% CO_2 and 1.5% H_2S,

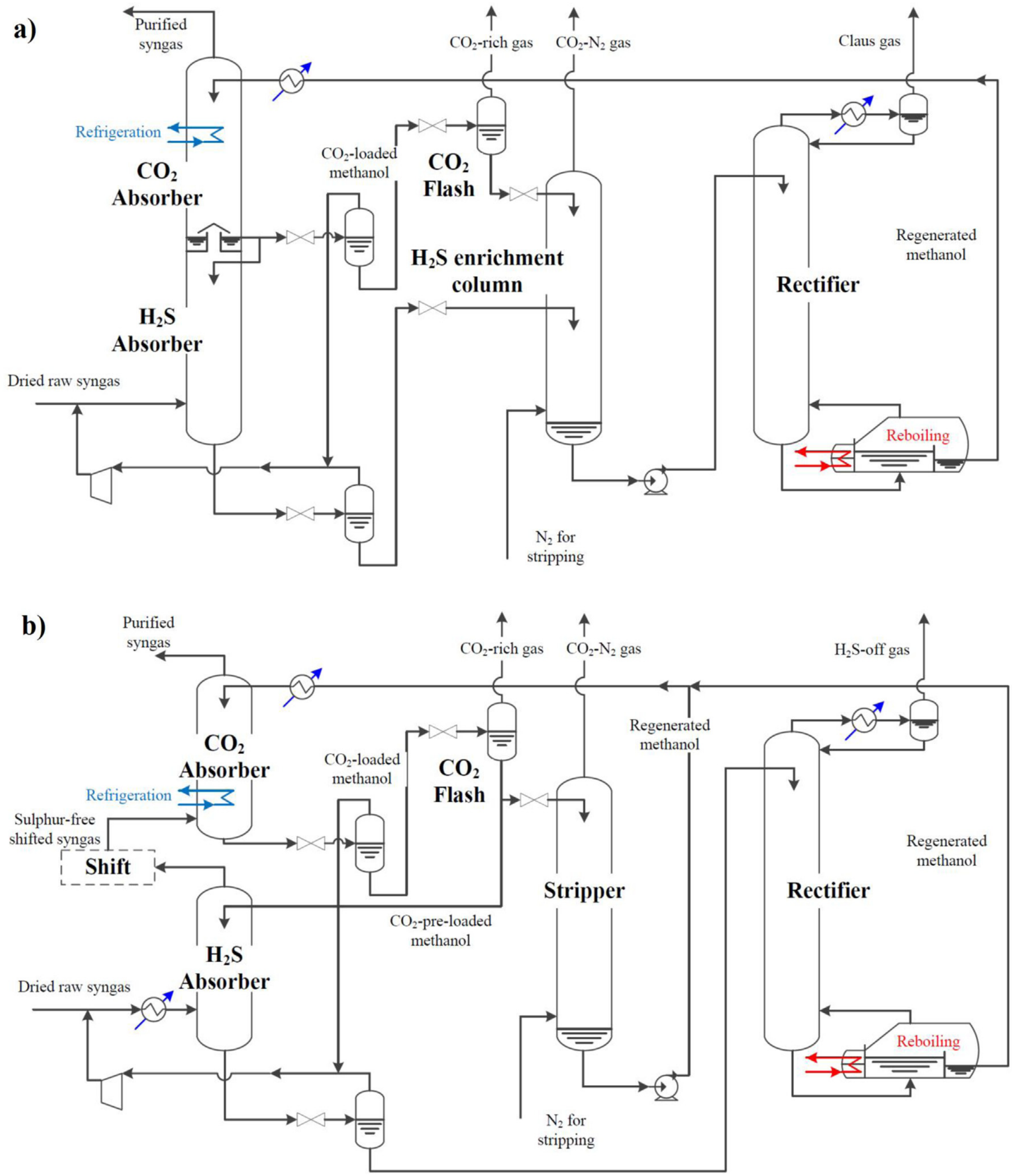

Fig. 2. a) One-stage and b) Two-stage Rectisol® scheme, adapted from Refs. [20] and [21].

directly to the environment [14]. To date, AirLiquide-Lurgi has built more than 85 Rectisol® plants [15] and Linde more than 65 [16]. According to Koss [17], 75% of the syngas capacity produced worldwide from coal, oil residues or waste, is purified by a Rectisol® unit. The features making Rectisol® the most popular AGR technology for gasification-based syngas cleaning are (1) the capacity to deeply remove trace contaminants potentially harmful to down-stream processes like COS (without requiring an hydrolysis unit), HCN, NH_3, metal carbonyls and possible aromatic hydrocarbons, (2) the possibility to reach a wide range of H_2S and CO_2 separation levels, and (3) the adaptability of the layout to meet almost any specific upstream syngas condition as well as downstream product specification. The Rectisol® process can be tailored for a large variety of applications comprising syngas to power (IGCC), Coal to Liquids (CTL), Coal to methanol, ammonia and chemicals in general. Moreover, its design can be arranged to perform either a combined (one-column) or selective (two-columns) removal of H_2S/COS and CO_2. In addition, the layout can be tuned to match the water gas shift configuration placing the CO_2 absorber upstream (for plants with sweet WGS) or downstream of the H_2S absorber (for plants with sour WGS).

Although Rectisol® may appear as an established old-fashioned process, its application to CCS is quite recent and may suggest a different process arrangement (as found in Ref. [1]) compared to more classical applications where most of the CO_2 stream is vented and not targeted to meet the tight specifications for CCS and EOR [18]. For the above-listed reasons, it is interesting to carry out a comprehensive analysis and investigate novel

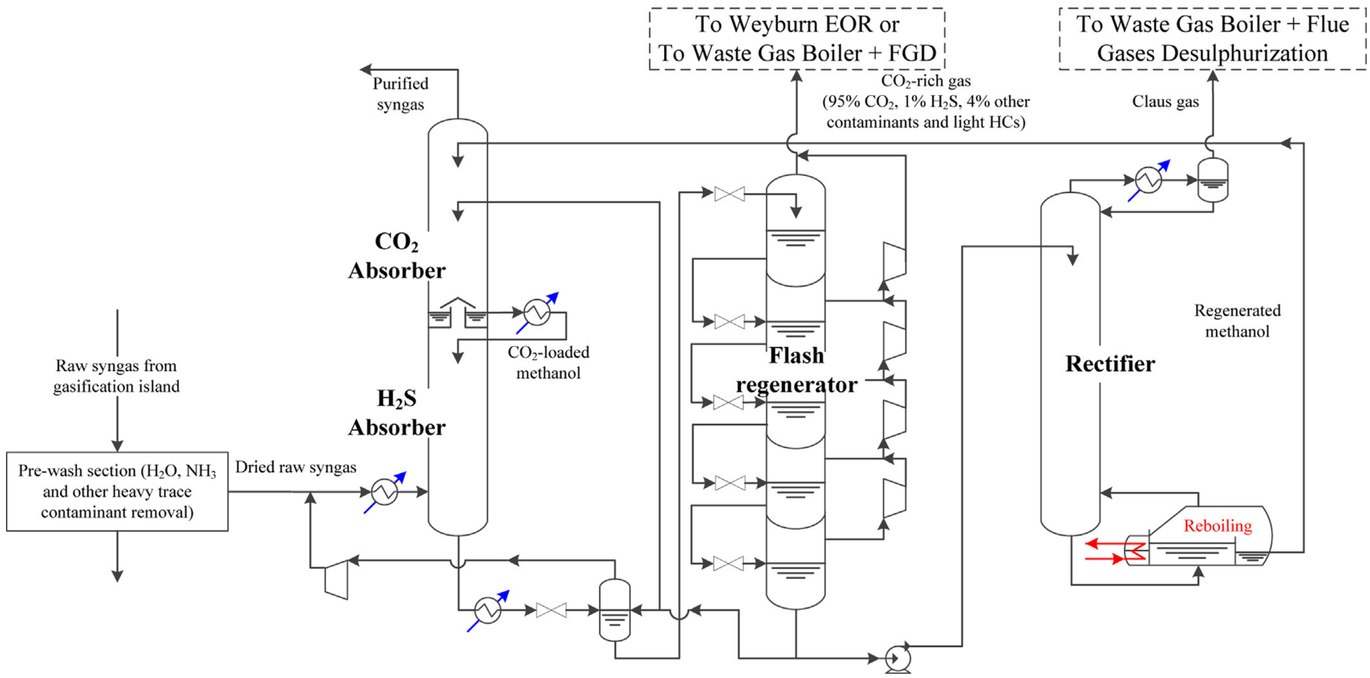

Fig. 3. Great Plains Synfuels Plant Rectisol® scheme adapted from Ref. [13].

options of Rectisol®-based processes for the selective removal of H_2S and CO_2.

In this work, first we make a brief review of the Rectisol®-based variants with the purpose of determining the best one for CCS (see Section 2). Then, we discuss the main issues related to the modeling and simulation of the process, and compute the performance of a reference scheme (see Sections 3 and 4). Subsequently, we describe an effective Heat Integration methodology and apply it to carry out the thermodynamic analysis of the reference scheme (see Section 5.1). Finally, on the basis of the observations and insights derived from the analysis of the reference scheme, we propose 4 novel schemes with optimized Heat Integration and lower energy con-sumption (see Section 5.2).

2. Review of the Rectisol® schemes for CCS

In this section, we first introduce the basic principles of the originally patented processes, then we make a brief review of the Rectisol® schemes suitable for CO_2 capture.

Methanol (MeOH), an alcohol with chemical formula CH_3OH classifiable as a polar protic solvent, is capable of preferentially dissolving H_2S and CO_2. As a result, it can selectively remove those two acid gases from a syngas stream. It is not the most selective solvent, as Selexol® has a higher selectivity, as shown in Ref. [13]. However, compared to Selexol®, it has two important advantages: (1) solubilities of H_2S and CO_2 considerably increase at low temperatures [13], (2) it can operate at very low temperatures (i.e., 213 K) to boost its methanol acid gas solubility and, in turn, decrease the solvent flow rate and absorber size. Other advantages of methanol are the capacity of removing multiple contaminants at once (e.g., HCN, NH_3, Carbonyls), low viscosity, low-corrosivity and non-foaming tendency.

The Rectisol® processes originally patented by Lurgi and Linde are represented in Fig. 1a) and b).

Lurgi's scheme [11], which essentially coincides with the one operating in the largest Sasol CTL plant in South Africa [14], includes a pre-washing column for water, hydrocarbons and heavier contaminants removal (which can have a separate solvent circuit) followed by the absorption column in which two chilled methanol streams at 223 and 213 K wash the CO_2, H_2S and COS out from the syngas. The bottom of the column is externally refrigerated with an ammonia refrigeration cycle. The loaded liquid methanol is then regenerated by flashing to atmospheric or sub-atmospheric pressure and, partly, by distilling the small fraction which is then introduced in the absorber from the top stage. On one hand, this solution, in which the washing agent is purified mainly by pressure reduction, is simple (just one absorption column, a flash column and a regenerator) and with a limited energy consumption, thanks to the auto-refrigeration effect associated to the expansion; on the other hand, it is not selective and it turns out to be unsuitable for CCS, since the CO_2 gas released from the flash (corresponding to 98% of the total CO_2 contained in the raw syngas) contains about 1.5% of H_2S (two orders of magnitude larger than the acceptable limit for EOR) and would need an additional complex and expensive chemical process to reach the required purity [14].

Linde's scheme [12] of Fig. 1b) is more suitable for CCS, since it is selective and produces a CO_2-rich stream readily available for either EOR or urea production. In this arrangement, the absorber is inter-cooled to remove part of the heat of absorption of CO_2 and features an intermediate extraction of almost half of the solvent flow rate at the exit of the CO_2 removal section of the column. In the H_2S absorber, located at the base of the column, the already CO_2-satu-rated methanol removes the H_2S from the rising raw syngas. The liquids collected at the bottom of the absorber go through a pre-flash to recycle the most volatile fuel species and are then sent to an H_2S enrichment column. Most of the CO_2 is released in the H_2S enrichment column, whereas the remainder is desorbed in a N_2 stripper.

This flowsheet makes available 86.6% of the inlet CO_2 as a pure stream (98.6% purity) at 3 bar suitable for CCS, about 10% in the diluted tail, and 3% in the Claus gas [19]. Compared to the case of Fig. 1a), this solution is readily adaptable to CCS with minor modifications, even though it adopts desorption pressures not optimized for this purpose. Moreover, the N_2 diluted stream of CO_2, featuring a concentration unsuitable for CO_2 capture, is detrimental because it limits the maximum achievable CO_2 Capture Level (CCL). It is worth emphasizing that, as also reported in Ref. [1], this scheme was not supposed to be used for CO_2 capture but just for a partial utilization of the separated CO_2 for urea synthesis. This configuration is claimed by the inventors to be appropriate for providing a Claus suitable stream containing 40% (molar basis) of H_2S when starting from a syngas with a medium/high H_2S content (the patent provide the example for a case with 0.6% of H_2S in the dry raw syngas deriving from the gasification of bituminous coal or petcoke). If the syngas has a much lower H_2S concentration (e.g. 0.1% molar basis or lower), it is recommended to rearrange the H_2S enrichment section (i.e., CO_2 desorption section) by adding downstream of it and upstream of the methanol regenerator a rectification column followed by an additional scrubber, as explained by the same authors [12].

Hochgesand [20] and Weiss [21] proposed the scheme represented in Fig. 2a), very similar to the previously described one but with a slightly different arrangement of the H_2S enrichment section. It entails a flash of the CO_2-loaded methanol, which releases almost pure CO_2, followed by a column working as H_2S reabsorber in the upper section, and as a CO_2 stripper in the lower section. The "two-stage" variant of this scheme, proposed in Refs. [20] and [21], is shown in Fig. 2b). The H_2S and CO_2 removal columns are separated and the WGS unit (sweet catalyst) is placed in between them. This configuration is aimed at keeping as low as possible the CO_2 concentration within the H_2S absorber, in order to minimize the amount of captured CO_2 and then to avoid the H_2S enrichment column. Despite this positive effect on the H_2S/CO_2 selectivity, the scheme is more complex and rarely implemented as it shows higher investment costs (columns duplication with shift reactor in between) without a significant saving in energy consumption and operating costs.

Among the proposed configurations [21], highlights the attractiveness of the scheme with "two-parallel-absorbers" for plants in which a shifted and an unshifted stream must be scrubbed, like for instance CTL and Coal to SNG plants. Indeed, since only a partial WGS conversion is required, a fraction of the syngas stream

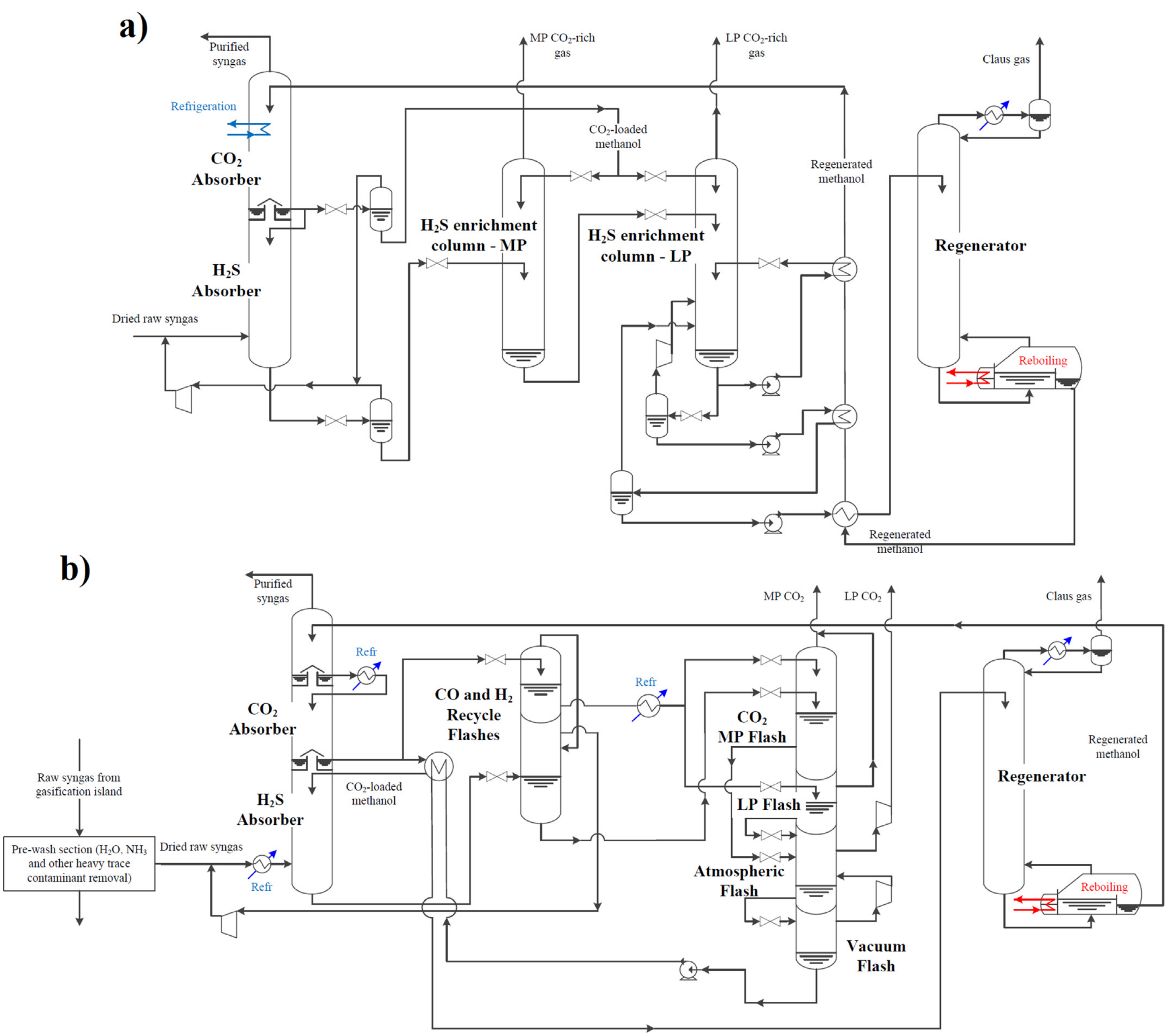

Fig. 4. a) Linde (adapted from Ref. [25]) and b) Lurgi (adapted from Ref. [26]) Rectisol® scheme for CCS.

bypasses the WGS unit. In the "two-parallel-absorbers" Rectisol®, the shifted branch goes through a traditional Rectisol® (the one shown in Fig. 1b)), whereas the bypass stream (un-shifted) goes through an H_2S absorber column. The AGR units of the two branches share the solvent regeneration section. The energy consumption of the scheme is reduced since it benefits from a higher CO_2 concentration in the shifted branch. On the other hand, this option has a higher plant complexity and it fails to provide a CO_2 stream with a concentration satisfactory for CO_2 capture. Indeed, according to [21] the stream of captured CO_2 contains 17% (molar basis) of impurities (mostly N_2).

More recently, a comparison between a traditional (single-stage) Rectisol® and a double-stage one has been carried out in Ref. [22]. Their analysis, based on process simulations and Heat Integration techniques, shows that the refrigeration power of the single-stage option is just 35% of that of the double-stage case, confirming the superiority of the former both from the point of view of energy penalty and capital costs.

In Ref. [23] the performance of a simplified Rectisol® is compared to that of other physical and chemical solvent-based Acid Gas Removal processes. The analysis is based on process simulation and assumes as case study a 50 MWth Coal to SNG plant. The au-thors highlight the considerable effect of heat integration on the energy consumption of the Rectisol® process.

Among the existing plants, the Great Plains Synfuels Plant [24] (owned by the Dakota Gasification Company) operates a Rectisol® (built by Lurgi) that, since 2000 has sold 60% of the total CO_2 generated as a byproduct to the Weyburn EOR project, making the plant one of the first energy facilities anywhere to sequester CO_2. Its simplified flowsheet is reported in Ref. [13] and is shown in Fig. 3. Like the Sasol-CTL Rectisol®, this scheme is based on desorption via a sequence of six flashes and is conceptually similar to the Lurgi patent of Fig. 1a).

Unfortunately, the CO_2 stream produced by the plant is quite contaminated, since it contains 1% of H_2S and 4% of hydrocarbons and, therefore, does not satisfy the recent guidelines for CCS and EOR. Moreover, similarly to what happened in above-mentioned Sasol facility, most of the measures for reducing the H_2S content in the CO_2 stream failed (Stretford, Sulfolin and other H_2S removal processes) due to operational difficulties [24].

The previously cited drawbacks spurred the designers to propose variants of the Rectisol® configuration in order to make it suitable and effective for CCS. To this purpose, both Linde [25] and Lurgi [26] have recently proposed flowsheets for the selective removal of H_2S and CO_2 with high CO_2 capture rates (see Fig. 4a) and b)) where CO_2 is released at different pressures in two sequential desorption columns (replacing the original H_2S enrichment section).

Munder et al. [25] developed the scheme reported in Fig.4a). The design maintains the same MP-regeneration column of Fig. 1b) and replaces the N_2 stripper with a more complex LP-column combining CO_2 desorption by flashing and heating with H_2S re-absorption via methanol recirculation. The Reference scheme adopted in the present study (see Section 4) is thought to resemble this solution.

Kasper [26] proposed the arrangement shown in Fig.4b). Similarly to the Great Plains Synfuels plant, it exploits four sequential flashes, the last being sub-atmospheric, to make available two purified streams ready for compression and sequestration. In this case, the process takes advantage of the auto-refrigeration effect provided by CO_2 desorption from the solvent. Nevertheless, this solution is penalized by the relatively low CO_2 release pressures (the last one is sub-atmospheric) which leads to a high power consumption of the CO_2 compression unit. This impact is often neglected or underestimated, since the CO_2 compression unit is frequently not included in the energy consumption of the AGR process. As a result, the AGR flowsheet is often tuned and optimized without considering the effects on the power consumption of the CO_2 compressor.

Moreover, it is worth noting that none of the above-listed works pays particular attention to the energy analysis and Heat Integration of the process. Moreover, the most energy intensive utilities, namely

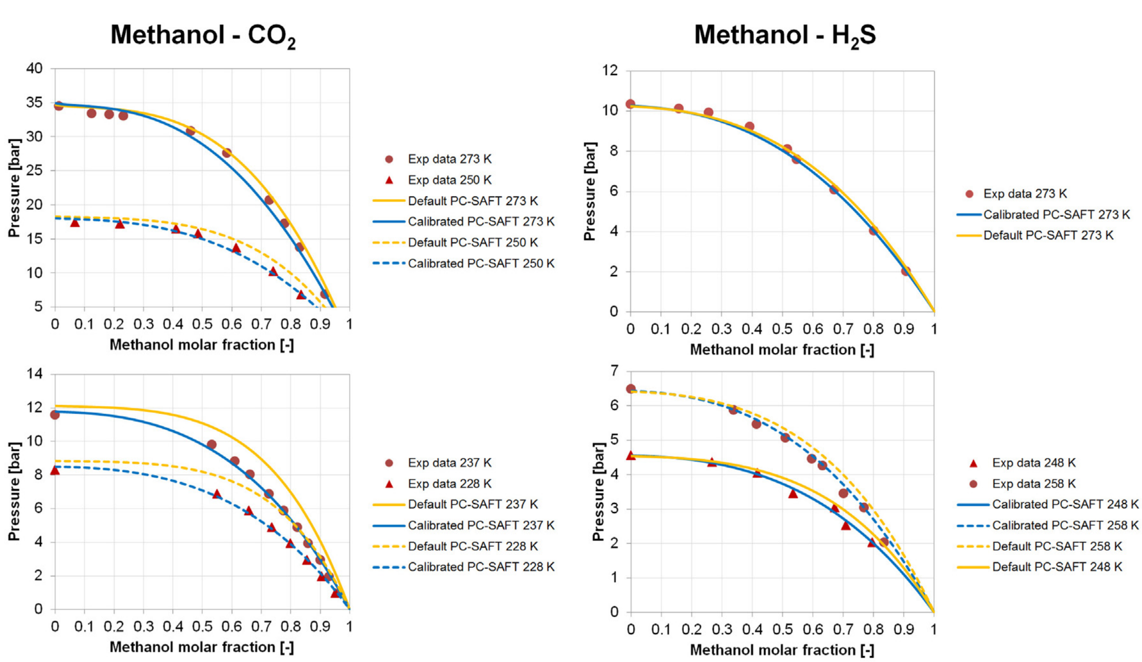

Fig. 5. Bubble point curves at constant temperature for Methanol-CO_2 and Methanol-H_2S mixtures at conditions representative of a Rectisol®-based process. The experimental points are in red, the values obtained with the calibrated EOS are in blue and the value resulting from the Aspen default are in yellow. (For interpretation of the references to colour in this figure legend, the reader is referred to the web version of this article).

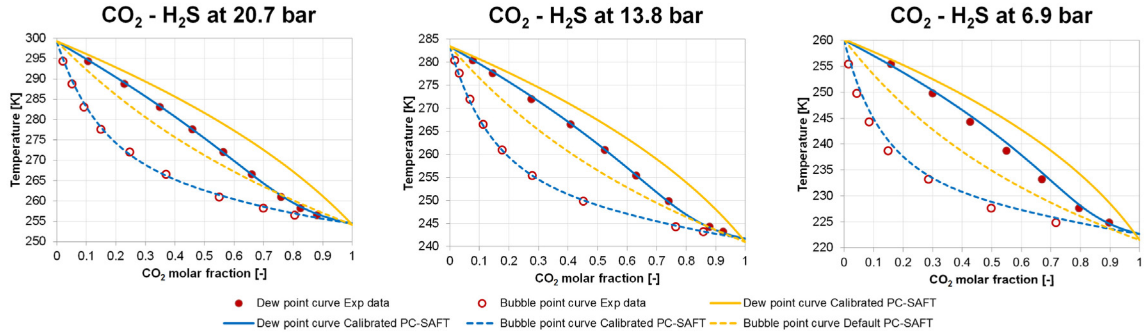

Fig. 6. Bubble and dew point curves at constant pressure for the CO_2—H_2S pair at conditions representative of a Rectisol®-based process. The experimental points are in red, the Values obtained with the calibrated EOS are in blue and the value resulting from the default EOS of Aspen are in yellow. (For interpretation of the references to colour in this figure legend, the reader is referred to the web version of this article).

the CO_2 compressor, the refrigeration cycle, and the steam needed by the reboilers, are usually left outside the analysis or designed separately, therefore missing any possible thermodynamic benefit or synergy deriving from a better integration with the process.

3. Equation of state

The Rectisol® process entails physical transformations at relatively high reduced pressures and low reduced temperatures for the acid gases to be separated (i.e., close to the critical point for CO_2 and H_2S). As a consequence, in the physical absorption and desorption of CO_2, H_2S and other species into methanol, as well as in the heat exchangers with phase-changes and in the CO_2 compressor, the fluid behavior is far from ideal. For these reasons, in order to build an accurate model of the Rectisol® process, it is necessary to select and calibrate the proper equation of state (EOS).

Ideally, the most accurate EOS should, on one hand, have a strong theoretical foundation to ensure a good predictive capability, and on the other hand, include all the experimental data available for the mixture of interest. This has been done recently to describe the thermodynamic behavior of some common mixtures like dry air or natural gas. For instance, the main thermodynamic properties of air, in its real-gas region, can be accurately computed via a reference empirical multi-parameter EOS expressed in the form of a non-dimensional Helmholtz energy, as described in Ref. [27]. A similar approach is applied to natural gas mixtures (see the GERG-2008 EOS published in Ref. [28]).

Unfortunately, even though CH_3OH—CO_2—H_2S mixtures with H_2 and CO as major components are well-known, the available set of experimental data is not so extensive to justify the adoption and calibration of a specific reference EOS. As a result, we need to select the EOS among the available models looking for the following characteristics: (i) theoretical consistency, (ii) implementation in a process simulation software, (iii) computational time of Vapor-Liquid Equilibria (VLE) related properties, (iv) possibility to be tuned for the specific conditions of interest. We selected the PC-SAFT, a semi-empirical EOS developed on the basis of mechanical statistics models, already implemented in commercial flowsheet simulation codes (e.g., Aspen Plus® version 7.3 [29] by AspenTech used in this work), and capable of calculating the VLE properties of

Table 2
Operating conditions of the GE-Texaco gasifier and process specifications and assumptions.

Gasification island conditions			
As Received Coal Ultimate Analysis		Gasifier operating conditions	
C	63.8%	Gasifier type	GE-Energy with Radiant Syngas Cooler
H	4.1%	Gasification pressure, bar	40
O	6.5%	Syngas temperature at gasifier exit, K	1589
N	1.0%	Carbon conversion, %	99%
S	4.5%	O_2 purity, %mol	95%
Cl	0.1%	Coal/slurry ratio, %mass	66%
Moisture	2.5%	Temperature of O_2 to gasifier, K	443
Ash	17.7%		
LHV, MJ/kg	25.07		
Coal input (LHV),MW	1343.1		
AGR conditions			
Raw Syngas Inlet		Products specifications	
Mole Frac		CO_2 captured	
CO_2	28.0%	CO_2CL, %	98%
H_2S	1.3%	CO_2 purity, %mol	>97%
CO	23.4%	H_2S fraction, ppmv	<150
N_2	0.4%	Pressure, bar	150
H_2	46.9%	Temperature, K	298
CH_4	0.0%	Clean Syngas	
Total Flow, kmol/sec	5.404	Pressure, bar	30
Total Flow, kg/sec	110.2	H_2S fraction, ppbv	<50
Temperature, K	303	Stream processed by Claus	
Pressure, bar	35	H_2S/CO_2 ratio, –	>1/5
		CO_2 in the Claus tail gas	Recycled to the AGR absorption section

Table 1
Value of the binary interaction parameter for the most relevant binary mixtures involved in a Rectisol®-based acid gas removal systems.

Component i	CH_3OH	CH_3OH	CH_3OH	CH_3OH	CO_2	CO_2	CO_2
Component j	CO_2	H_2S	H_2	CO	H_2S	H_2	CO
Number of exp data used	81	36	39	14	45	46	21
Temperature range, K	213–288	248–298	243–298	298–323	223–298	220–270	223–263
a_{ij}	−0.0039	0.0022	−0.0642	−0.0321	−0.0055	0.0371	0.0012
b_{ij}	0.0216	−0.0228	−0.2374	0.0603	0.0821	−0.5063	−0.0339
c_{ij}	0.0392	−0.1233	−0.546	−0.1097	0.1437	−0.2855	0.1094
T_{ref}, K	298.15	298.15	298.15	298.15	298.15	298.15	298.15
AAD NEW	6.1%	6.6%	3.8%	3.8%	1.7%	9.6%	3.1%
AAD DEFAULT ASPEN	12.6%	8.8%	29.9%	18.3%	16.6%	54.3%	14.6%

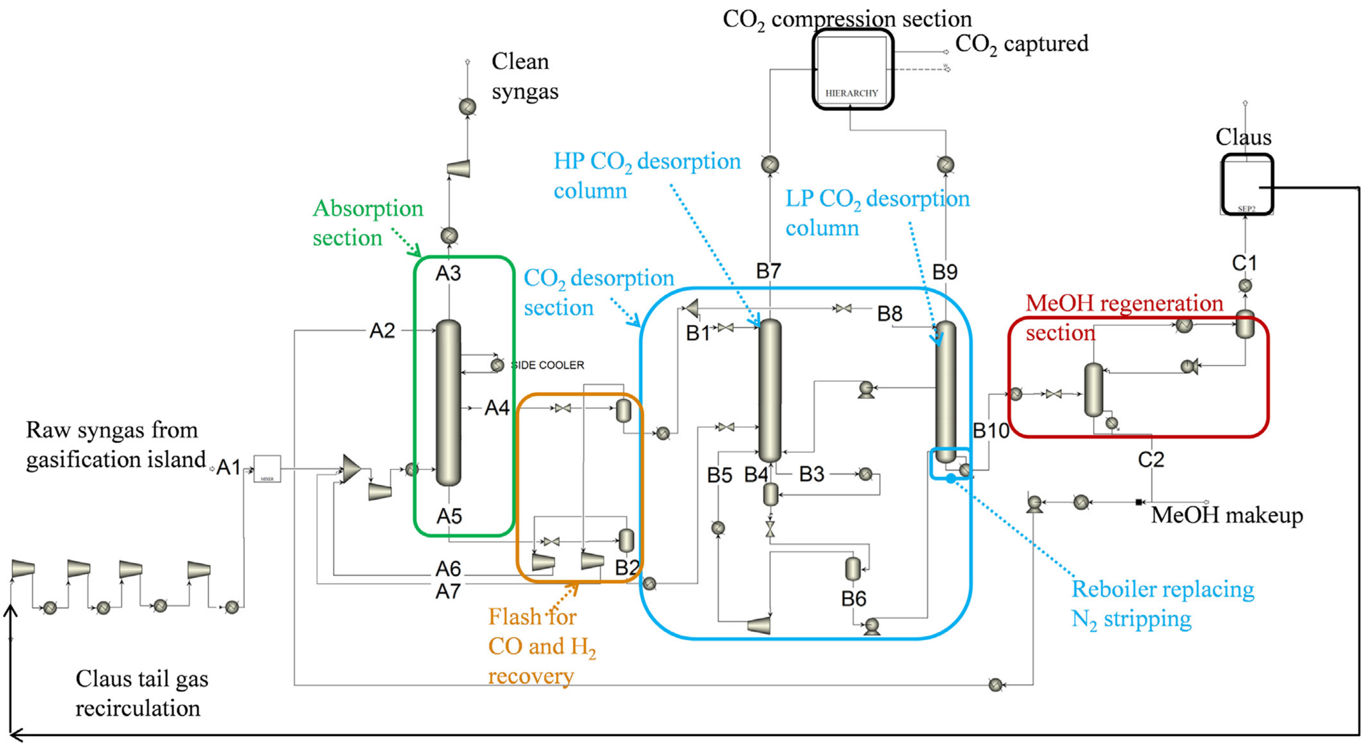

Fig. 7. Rectisol® scheme implemented in Aspen Plus® and adopted as Reference configuration for the analysis.

the mixtures of interest with reasonably short computational times (e.g., it is possible to calculate an absorption column in less than 0.1 s on a common desktop PC, and an entire Rectisol® flowsheet in 10–60 s depending on the accuracy of the initial solution), and including a set of binary interaction parameters which can be adjusted to improve the model accuracy in a specific region of pressures, temperatures and compositions. As shown in Ref. [30], the PC-SAFT can be adjusted to predict the VLE of mixtures by calibrating the binary interaction parameters. Practically, a binary interaction parameter is a fully empirical coefficient (i.e., without any theoretical foundation), introduced to improve the matching of the VLE curves for each binary mixtures of interest. It is worth mentioning that, in order to improve the regression accuracy of the experimental data, these coefficients can be considered as functions of temperature. Of course, if this expedient is used, the EOS is supposed to be used only in the temperature range of calibration (avoiding extrapolation).

As a matter of fact, also the cubic-type EOSs share most of the previous features with PC-SAFT. Nevertheless cubic EOSs incorporate less theoretical information than PC-SAFT (which includes three molecular based parameters for each pure substance), and we found out that, even after a careful calibration, they showed a slightly lower accuracy than PC-SAFT in the calculation of both VLE and volumetric properties in single phase regions. It is worth noting that recently also Diamantonis et al. ([31] about CO_2 mixtures with other gases and [32] specific to CCS applications) and Sun and Smith [22] adopted the PC-SAFT EOS highlighting its suitability for modeling CCS systems and Rectisol®-based processes. Sun and Smith [22] provide updated calibration parameters for the binary pairs $CH_3OH{-}CO_2$ and $CH_3OH{-}H_2S$ obtained on the basis of experimental data [33] and [34]. Their model correction is focused on the reconciliation of the thermodynamic properties of the streams entering and exiting the absorption section of a Rectisol® plant [35].

Table 3
Main assumption of the Aspen Plus® model of the Reference Rectisol® process.

Heat exchangers			Process expanders/compressors/pumps		
Pressure loss	%	2	Isoentropic efficiency of syngas expander	%	88
$\Delta T_{MIN}/2$ for process streams/refrigerator/cooling water	K	5	Polytropic efficiency of syngas compressor	%	84
$\Delta T_{MIN}/2$ for reboiler utility	K	10	Pressure ratio	–	<3
ABSORPTION/STRIPPING COLUMNS			Mechanical/Electric efficiency	%	92
Model type	–	Radfrac (equilibrium)	CO_2 COMPRESSOR		
Column type	–	Tray	Number of stages	–	5 (+1 pump)
N equilibrium stages H_2S absorber	–	10	Final delivery pressure	bar	150
N equilibrium stages CO_2 absorber	–	4 + cooler + 4	Pump inlet pressure	bar	80
N equilibrium stages CO_2 desorber HP	–	20	Compressor polytropic efficiency	%	84
N equilibrium stages CO_2 desorber LP	–	15	Final pump hydraulic efficiency	%	78
N equilibrium stages methanol regenerator	–	10	Temperature at intercooler exit	K	298
			Pressure drops intercooler and dryer	%	2
Minimum allowed temperature for CO_2 rich vapor streams	K	217	Drivers Mechanical/Electric efficiency	%	92

Table 4
Stream tables of the Reference Rectisol® process.

Steam ID	A1	A2	A3	A4	A5	A6	A7	B1	B2	B3	B4	B5	B6	B7	B8	B9	B10	C1	C2
Property																			
Mole %																			
CH_3OH	0.0%	100.0%	0.0%	79.8%	71.7%	0.1%	0.1%	82.0%	74.0%	84.9%	0.2%	0.2%	93.6%	0.0%	82.0%	0.0%	94.8%	0.2%	100.0%
CO_2	28.0%	0.0%	0.7%	18.9%	25.4%	64.2%	62.4%	17.7%	24.1%	13.7%	96.4%	94.7%	5.3%	98.4%	17.7%	98.9%	4.2%	80.6%	0.0%
H_2S	1.3%	100 ppb	16 ppb	55 ppm	1.6%	1.4%	63 ppm	55 ppm	1.6%	1.4%	3.4%	5.1%	1.0%	106 ppm	55 ppm	661 ppm	1.0%	19.3%	100 ppb
CO	23.4%	0.0%	32.7%	0.7%	0.7%	17.5%	18.4%	0.2%	0.2%	0.0%	0.0%	0.0%	0.0%	1.1%	0.2%	0.7%	0.0%	0.0%	0.0%
N_2	0.4%	0.0%	0.6%	0.0%	0.0%	0.3%	0.4%	0.0%	0.0%	0.0%	0.0%	0.0%	0.0%	0.0%	0.0%	0.0%	0.0%	0.0%	0.0%
H_2	46.9%	0.0%	66.1%	0.6%	0.6%	16.4%	18.7%	0.1%	0.1%	0.0%	0.0%	0.0%	0.0%	0.4%	0.1%	0.3%	0.0%	0.0%	0.0%
Total flow kmol/sec	5.40	6.51	3.83	4.08	4.54	0.14	0.11	3.57	4.39	7.66	0.24	0.47	6.95	1.40	0.40	0.10	6.86	0.36	6.51
Total flow kg/sec	110.17	208.54	41.88	139.11	158.41	4.94	3.67	121.90	153.47	258.30	10.45	20.55	227.30	61.08	13.54	4.39	223.45	14.95	208.50
Temperature C	30.0	−50.0	−45.2	−4.4	−11.8	35.1	44.7	−45.0	−14.2	−23.5	−17.0	20.0	−32.1	−34.4	−51.3	−49.9	−14.2	20.0	69.6
Pressure bar	35.0	60.0	60.0	60.0	60.0	35.0	35.0	19.8	20.0	6.0	6.0	6.0	2.0	6.0	2.7	2.7	2.7	1.2	1.2

In this work, we provide updated calibration parameters not only for the binary pairs CH_3OH—CO_2 and CH_3OH—H_2S, but also for the CH_3OH—CO, CH_3OH—H_2, CO_2—H_2S, CO_2—H_2 and CO_2—CO couples. Compared to the work of Sun and Smith [22] which is focused on the absorption section of a specific Rectisol® design, we aim at providing a set of calibrated binary interaction parameters that can cover the typical composition, temperature and pressure ranges of a whole Rectisol®-based flowsheet. The calibration was performed by means of the following steps:

- Selection of the most relevant binary pairs to be calibrated
- Identification of the temperatures and composition ranges of interest (the pressure range of the bubble and dew points is therefore a consequence of this choice)
- Collection of the VLE experimental data available from the NIST ThermoData Engine [36]
- Formulation of the EOS calibration problem as a non-linear constrained optimization program whose objective function is the mean average error on the saturation pressure in absolute value (AAD, as expressed in Eq. (1)), and whose variables are the three coefficients (a_{ij}, b_{ij} and c_{ij}) defining the binary inter-action parameters k_{ij} [30] as a function of the temperature (see Eq. (2)).

$$AAD = \left|\frac{p - p_{\mathrm{ref}}}{p_{\mathrm{ref}}}\right|, \tag{1}$$

$$k_{\mathrm{ij}} = a_{\mathrm{ij}} + b_{\mathrm{ij}}\frac{T\mathrm{ref}}{T} + c_{\mathrm{ij}}\ln\left(\frac{T}{T\mathrm{ref}}\right). \tag{2}$$

The unconstrained nonlinear optimization problem was solved with the derivative-free Simplex method available in MATLAB® R2012a (Mathworks [37]). We adopted a derivative-free method rather than a gradient-based one (such as sequential quadratic programming algorithms whose convergence rate is proven to be much faster than that of derivative-free methods) because the VLE calculation algorithm fails to reach convergence (hence it does not return a solution) for certain values of pressures and temperatures and this discontinuity cannot be handled by gradient-based algorithms.

The details about the experimental data used for the calibration and the optimized EOS coefficients are reported in Table 1. The last two rows of Table 1 compare the mean average error AAD of the calibrated EOS with that of the default PC-SAFT EOS available in Aspen Plus®. Fig. 5 reports an example of the results obtained for the methanol-acid gases pairs at the typical conditions of the absorption columns. Fig. 6 highlights on a Txy (i.e. at constant pressure) plot for the CO_2—H_2S mixture the improvement introduced by the calibration compared to the default EOS of Aspen Plus® (i.e., no binary interaction parameter for this specific couple).

4. Reference scheme and process model

In this section we present, simulate and analyze from a thermodynamic point of view a Rectisol® process tailored for CTL plants

Table 5
Main performance indexes of the Reference Rectisol® process.

Quantity	Units	Value
Electric consumption of Compressors	MW	29.2
Net Refrigeration duty (thermal)	MW	27.0
Electric consumption of Refrigerator	MW	21.1
Overall Reboiler duty (thermal)	MW	27.4
CO_2 Capture Level	%	97.5%

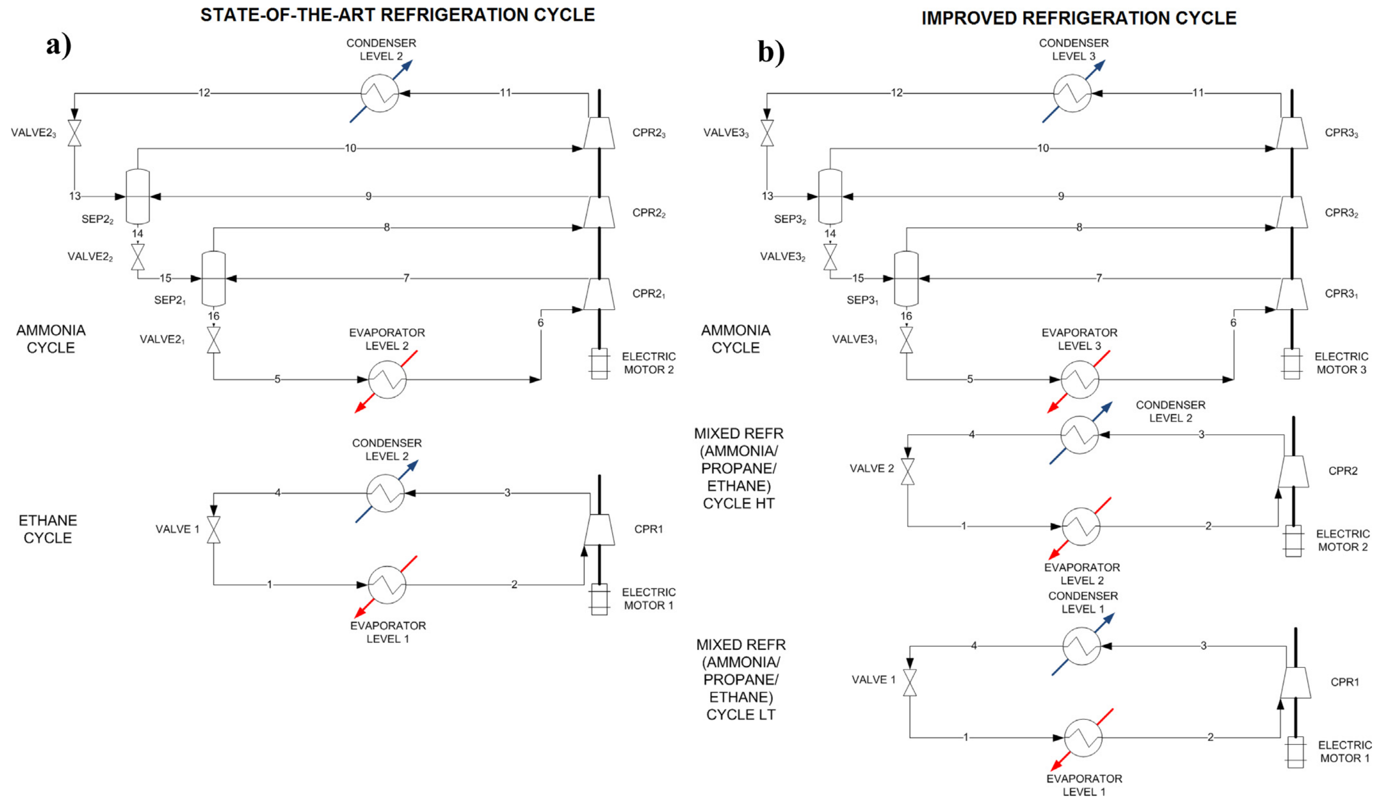

Fig. 8. Refrigeration cycles option considered in this study. a) State-of-the-art two cascade levels cycle with pure refrigerants. b) Improved three cascade levels cycle featuring mixed refrigerants in the low-temperature levels.

with CCS. More in detail, we consider the typical composition of a syngas stream generated by a GE-Texaco gasifier, whose operating conditions are reported in Table 2, followed by a WGS unit tuned to achieve a H_2/CO molar ratio equal to 2 (as required by a Co-based FT catalyst [38]). Similarly to the CCS plants in operation, it is assumed that the CO_2 stream is used for EOR, then its composition must meet the specification reported in Table 2 [18].

On the basis of the analysis conducted in Section 2, we developed the Rectisol® flowsheet represented in Fig. 7 which is an adaptation of the layout patented in Ref. [19]. Compared to the original design, the proposed flowsheet performs the CO_2 desorption from the liquid phase in the low pressure desorption column by reboiling rather than by stripping with N_2. This modification is introduced in order to produce a CO_2-based vapor stream with a composition suitable for CCS.

The absorber column is actually divided in two sections: the bottom part, here called the "H_2S absorber", where essentially all the H_2S is removed, and the upper part, the "CO_2 absorber", where the remaining CO_2 is absorbed. Raw syngas (A1) enters the bottom of the H_2S absorber while a fraction of the pre-loaded solvent flows down from the CO_2 absorber. The H_2S absorber, being fed with solvent pre-loaded with CO_2, minimizes the amount of absorbed CO_2. The CO_2 absorber is fed with lean methanol at the top (stream A2) and (almost) H_2S-free syngas at the bottom (coming up from the H_2S absorber). As a result, the liquid stream exiting the H_2S absorber (stream A5) contains almost all the captured H_2S and a relatively small amount of CO_2, while the liquid stream extracted from the bottom of the CO_2 absorber (stream A4) is almost sulphur-free and rich of CO_2.

As shown in Fig. 7, the CO_2 absorber has a side cooler to remove a fraction of the heat of absorption (i.e., heat released by the CO_2 as a consequence of the phase-change) by cooling the liquid stream to 248 K. The absorption takes place at 60 bar, a typical value ([39]) for Rectisol®. The absorption column could have an even more complicate configuration, for instance with a higher number of side coolers, but this expedient may cause a considerable increase in capital cost. The purified syngas exiting from the top of the absorber (A3) provides cooling and mechanical power via two heaters and one expander that bring it to the delivery conditions of 298 K and 30 bar. Streams A4 and A5 are then adiabatically flashed in order to vaporize and recycle down to the column inlet the more volatile fuel species, mostly H_2 and CO, that have been co-absorbed with acid gases. The two liquid streams exiting the flash section are then sent to the CO_2 desorption section whose goal is to release a vapor-phase CO_2 stream with a limited content of impurities, especially H_2S, making it suitable for EOR. The CO_2 desorption section is made of two columns, the High Pressure (HP) and the Low Pressure (LP) desorption column. Both are fed at the top with the sulphur-free streams B1 and B8 (obtained by flashing stream A4) which, once flashed inside the column, release the CO_2. The regenerated solvent flows down and wash the lower stages (avoiding that H_2S exits at the top of the columns together with CO_2). The operating pressures of the HP and LP desorption columns are 6 and 2.7 bar, higher than the values of the patent (3 and 1.8 bar, respectively), to reduce the CO_2 compression consumption and to limit the H_2S desorption. Stream B2 (containing most of the H_2S removed) is partly vaporized and fed to the bottom part of the HP desorption column which behaves like a reboiled H_2S enrichment column, receiving heat from and using B4 and B5 as stripping streams. The cascade of flash drums to which the liquid stream B3 goes through is the same as reported in the Linde patent [19] and it is used to improve the CO_2/H_2S separation. The LP CO_2 desorption column works essentially like the HP one. Thanks to the lower pressure and the Kettle reboiler, it is capable of recovering further CO_2 from stream B6. This results into a higher CO_2 Capture Level and a higher H_2S concentration in stream C1 sent to the CLAUS unit.

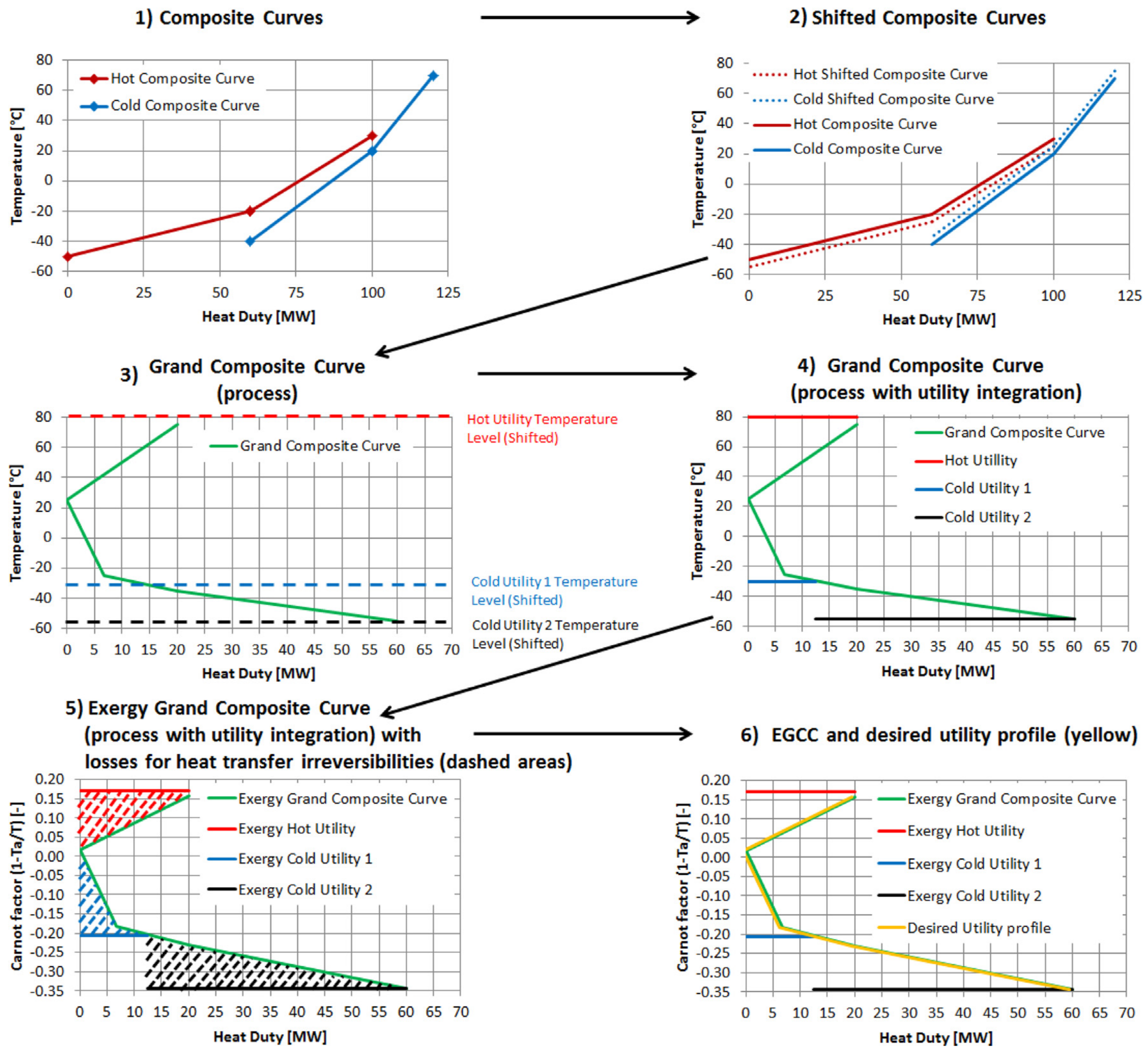

Fig. 9. EGCC construction procedure and meaning.

The CO_2 vapor streams produced by the CO_2 desorption section (streams B7 and B9) are then heated to ambient conditions so as to recover some refrigeration power and sent to a 5-stages intercooled compressor bringing the CO_2 to 80 bar. Finally, a pump stage pressurizes the CO_2 up to the capture condition of 150 bar. The H_2S-concentrated stream leaving the CO_2 desorption section (stream B10) enters the methanol regeneration column, a distillation column in which H_2S and the remaining CO_2 are stripped and sent to the CLAUS process (stream C1). The almost pure methanol stream is extracted (stream C2) at the bottom of the column. The process variables must be adjusted to obtain a molar concentration of H_2S in stream C1 above 20% so as to use a standard air fired CLAUS unit [1]. In the proposed flowsheet, the CLAUS unit is followed by an SCOT process which produces elemental sulfur and a

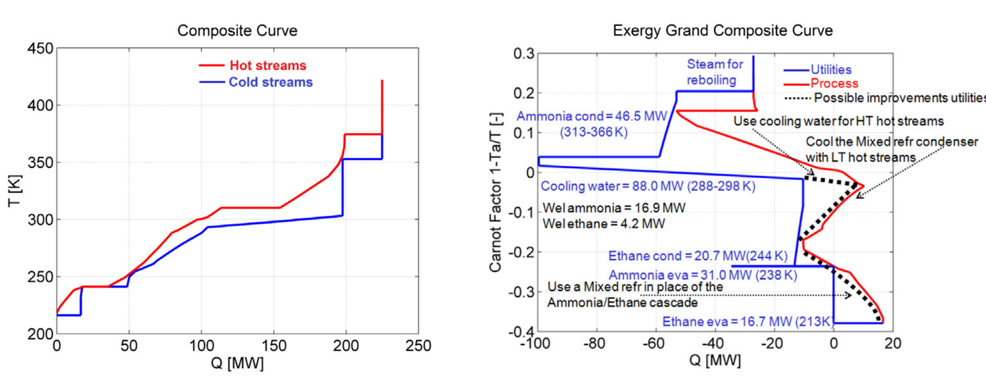

Fig. 10. CC and EGCC of the Reference case. Each curve is vertically shifted by $\Delta T_{min}/2$ in order to highlight the pinch points, i.e. $T_{corr} = T - \Delta T_{min}/2$ for hot streams and $T_{corr} = T + \Delta T_{min}/2$ for cold streams (Please note that there is no correnspondence between the colors of the EGCC and CC).

Table 6
Performance summary of the five configuration considered in this study.

Case		Reference	Scheme A	Scheme A mixed ref	Scheme B	Scheme B mixed ref
Absorption pressure	bar	60	60	60	60	60
Absorption temperature	K	223	223	223	223	223
CO_2 desorption pressure	bar	6.0/2.7	6.0/2.7	6.0/2.7	10	10
Methanol regeneration pressure	bar	1.2	1.2/0.7	1.2/0.7	1.2/0.7	1.2/0.7
CO_2 captured	kg/s	65.0	65.0	65.0	65.3	65.3
CO_2 Capture Level	%	97.5	97.5	97.5	98.0	98.0
Absorber raw syngas compressor (electric)	MW	12.3	12.3	12.3	12.1	12.1
Other process compressors/pumps (electric)	MW	8.0	8.0	8.0	11.4	11.4
Process expander (electric)	MW	−4.5	−4.5	−4.5	−4.5	−4.5
Net Reboiler duty from utility (thermal)	MW	26.0	5.7	5.7	6.2	3.2
Reboiler steam pressure	bar	1.5	0.5	0.5	0.5	0.5
Net Refrigeration duty (thermal)	MW	27.0	27.0	27.0	17.6	17.6
Process compressors/expanders electric power	MW	15.8	15.9	15.9	18.9	18.9
CO_2 compression power	MW	13.4	13.4	13.4	10.3	10.3
Electric equivalent of Reboiler duty	MW	5.0	0.7	0.7	0.8	0.4
Refrigeration electric power	MW	21.1	21.1	14.2	14.2	12.1
Cooling water consumption (electric)	MW	1.5	1.2	1.0	1.0	1.0
Chemical exergy of co-captured fuel	MW	3.3	3.3	3.3	4.0	4.0
Overall equivalent electricity consumption	MW	60.1	55.5	48.4	49.3	46.6
Specific Electric Equivalent Consumption	kJ/kg_{CO2}	925	854	744	755	714
SEEC reduction compared to Reference	%	–	−8%	−20%	−18%	−23%

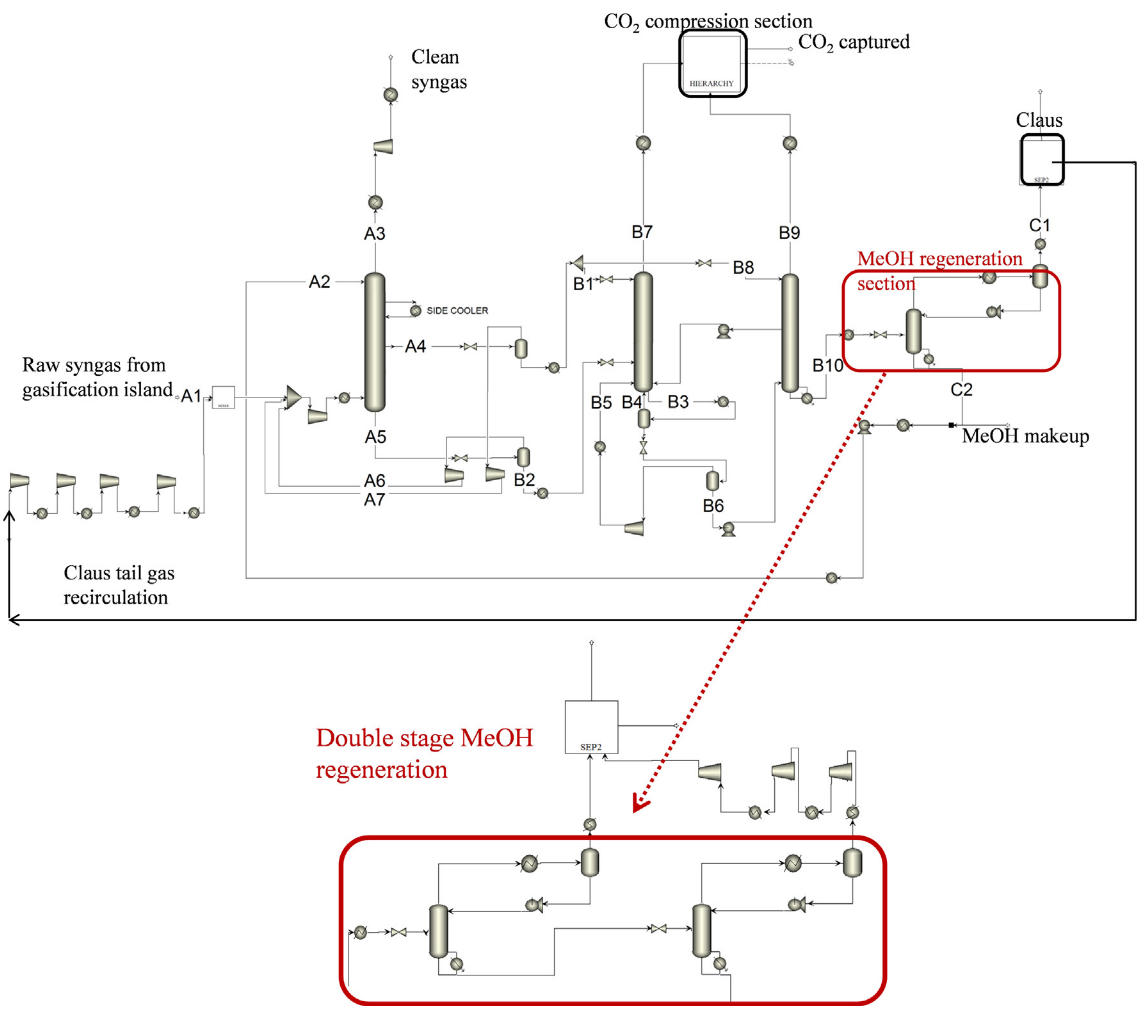

Fig. 11. Process flowsheet of scheme A, showing the details of the modified regenerator.

CO_2 rich tail gas which is recycled back to the Rectisol® inlet to maximize the CO_2 capture level.

The water removal system and the HCN, NH_3 and metal carbonyls pre-washer, which are among the features of the Rectisol® process, are not considered in this analysis because we assume that (1) these items are quite standard and (2) kept unchanged in all the variants herein considered (see Section 5), and (3) their designs do not significantly affect the performance of the Rectisol® process, as confirmed in Ref. [39]. Moreover, provided that for an entrained-flow gasifier, more than 97% of the sulfur from the coal is converted into H_2S (the remaining being mainly COS; see Ref. [14]) and that the solubility of H_2S and COS into methanol are very similar, we replace in the process model all the sulfur-based components with H_2S.

The flowsheet represented in Fig. 7 was modeled and simulated with Aspen Plus® version 7.3. The main calculation assumptions are reported in Table 3 while the stream tables are in Table 4 and the main performance indexes are in Table 5.

The performance summary reported in Table 5 highlights that the main energy consumption items affecting the efficiency of the process, listed in descending order, are (1) the electricity required to compress the CO_2 and the process streams (mainly the raw syngas compressor), (2) the refrigeration duty and (3) the reboiler duty. In the following sections we look for process modifications aimed at reducing those energy consumptions by applying the tools of Pinch Analysis.

5. Heat Integration and process improvements

The overall energy consumption of the Rectisol® process is made of the following items:

- $E_{Process}$, electric power absorbed by the process compressors and pumps,
- $E_{CO_2\ compr}$ electric power absorbed by the compressors and pumps of the CO_2 compression section,
- E_{Fuel}, chemical exergy (LHV basis) of the fuel species (mainly CO and H_2) co-captured with acid gases and sent either to storage or to the CLAUS,
- E_{Refrig}, electric power absorbed by the refrigeration cycle (cold utility),
- $E_{Cool\ wat}$, electric power required to circulate the cooling water (cold utility),
- $E_{Reboiler}$, electric power loss due to the extraction of steam from the steam cycle for the reboilers (hot utility).

Therefore, the overall energy consumption to be minimized is the sum of above-listed items including process units and utilities. More in detail, we considered the Specific Electric Equivalent Consumption (SEEC),

$$\mathrm{SEEC} = \frac{E_{CO_2\ compr} + E_{Process} + E_{Reboiler} + E_{Refrig} + E_{Cool\ wat} + E_{Fuel}}{m_{CO_2\ captured}} \left[\mathrm{kJ/kg}_{CO_2\ captured}\right] \tag{3}$$

where $m_{CO_2\ captured}$ is the mass flow rate of captured CO_2. $E_{Reboiler}$ is estimated on the basis of the mechanical power that the extracted steam could have provided to the steam turbine if it were expanded rather than extracted. More in detail, in order to estimate $E_{Reboiler}$, we assume a steam turbine inlet condition of 30 bar and 823 K, a condenser pressure of 0.05 bar, a turbine average isoentropic efficiency of 0.9, and that the steam extraction is at the pressure required by reboiler. It is worth noting that the mechanical power to heat ratio (w/q) turns out to be lower than the Carnot factor (defined as $1-T_a/T$, where T_a is the ambient temperature and T the saturation temperature of the steam stream considered). For instance, assuming to extract steam at 1.5 bar, the Carnot factor would be 0.251, whereas the w/q ratio is 0.192. For the same reason, $E_{Cool\ wat}$ is evaluated by assuming a typical value of 0.017 for the ratio between the electric power of the circulating pumps and the heat duty removed.

Such an approach is preferred to a method based on Carnot factors only (i.e., exergy analysis) because it estimates the actual electric consumption of the utilities.

While the energy consumption of the process units depends only on the process operative variables, that of the utilities is significantly affected by the Heat Integration, i.e., the arrange-ment of the process heat exchanger network (matching hot and cold process streams), the design of the utilities, and the inte-gration between process and utilities. It is worth noting that the Heat Integration plays a very important rule in low-temperature processes, like Rectisol®, because the exergy value of low-temperature thermal power is considerable, as described by Aspelund et al. [40]. For example, assuming an ambient temperature of 288 K, the exergy value of 1 MW thermal power at 268 K is 0.07 MW (7% of the energy, with a Carnot COP of 13.4), and 0.35 MW (35% of the energy, with a Carnot COP of 2.8) at 213 K.

5.1. Heat Integration methodology

Among the large number of Heat Integration techniques proposed since the 40's and reviewed in the recent book edited by Klemes [41], we adopted the "heat-cascade" methodology of Marechal and Kalitventzeff [42] as it allows to simultaneously optimize the process Heat Integration (i.e., determine the minimum energy requirement to be supplied by the utilities by properly matching hot and cold process streams) and the utility design (i.e., determine the utility type, operative variables, mass flow rates and size). Compared to other Heat Integration methods with Heat Exchanger Network synthesis, such as the classic mathematical programming techniques recently assessed by Escobar and Trierweiler [43], and that proposed by Salama [44], the methodology of Marechal and Kalitventzeff [42] allows to optimize the process Heat Integration and the utility design simultaneously, so as to exploit any possible synergy. Indeed, in this methodology, the utility streams are included in the heat cascade in order to allow for any possible integration options between process streams and utility streams. This method is currently implemented in the Osmose platform developed by LENI-EPFL [45]. According to this approach, the Heat Integration problem is formulated as a Mixed Integer Linear Problem having the following features:

- variables: mass flow rates of each of the available utilities, whose activation is defined by a related binary variable $y_i \in \{0, 1\}$ (equal to 1 if the i-th utility is used, 0 otherwise);

- objective function: minimize the exergy consumption of the utilities;
- constraints: heat balance for each temperature interval, while respecting the minimum temperature difference for each class of streams ΔT_{min}, according to the “heat cascade” methodology.

The MILP is solved with the free code GLPK [46]. Optionally the intensive operative variables of the utilities (i.e., pressures and temperature levels) can be optimized by adding an upper optimization level which runs the MILP model as a black-box function ([45]).

In this analysis we considered $\Delta T_{min}/2$ refrigerant = 3 K, $\Delta T_{min}/2$ hot utility = 10 K, $\Delta T_{min}/2$ process streams and cooling water = 5 K. The available hot utilities are assumed to be saturated steam at 3, 1.5 and 0.5 bar, whose w/q conversion factors (expressed as the ratio between the equivalent electricity loss and the heat provided) are respectively 0.242, 0.192 and 0.123. The cooling water is assumed to be available as a circulating loop operating between 288 and 298 K, and whose w/q conversion factor is 0.017.

Since the refrigeration cycle is expected to have the largest energy consumption, it has been accurately modeled and simulated with Aspen Plus® in order to get an accurate estimate of the electricity consumption. Two configurations are considered:

- A two-level cascade ethane/ammonia refrigeration cycle and is expected to represent a real, commercial refrigerator (see Fig. 8a))
- A three-level cascade cycle featuring two mixed refrigerant cycles as lower levels and an ammonia cycle as the top level (see Fig. 8b)). It is meant to represent a more complex refrigerator, specifically conceived to reduce the refrigeration power via a better matching with the process requirements.

We determined the optimal process Heat Integration according to the following procedure:

1. Simulate the process (i.e., solve the flowsheet) with Aspen Plus®,
2. Simulate the refrigeration cycle with Aspen Plus® for fixed intensive operative variables (i.e., pressures and temperature levels),
3. Extract the temperature–heat data of all the process streams and carry out the Heat Integration by solving the MILP problem,
4. Compute the SEEC with Eq. (3),
5. Analize the Composite and Exergy Grand Composite Curves of the system to identify the main sources of heat transfer irreversibility,
6. Figure out modifications of process and utilities which can improve the Heat Integration and/or reduce the energy consumption,
7. Repeat the procedure from step 1) for the new process/utility configuration

The Composite Curves (CC) are the well-known tool of Pinch Analysis used to analyze the Temperature–Heat Duty (T–Q) profile of processes [47], while the Exergy Grand Composite Curves (EGCC), proposed in Ref. [42], are obtained from CCs by reporting the heat surplus and deficit at each temperature level as a function of the Carnot factor, i.e., $1-T_a/T$, where the hot streams are shifted by $-\Delta T_{min}/2$, and the cold streams by $+\Delta T_{min}/2$, so as to highlight pinch points and making easier utility targeting. As a result, in an EGCC plot the area between the hot and cold curves corresponds to the exergy destroyed due to heat transfer irreversibility. Fig. 9 shows the steps followed for the construction of the EGCC, highlighting the exergy losses due to irreversibilities (dashed areas on the last graph). Moreover, from the EGCCs it is possible to deduce also the Minimum Energy Requirement for the hot and cold utilities. An example of EGCC referred to the process evaluated in this paper is reported in Fig. 10. For this reason, EGCC plots are ideally suited to identify and assess irreversibility sources in the integration between hot and cold streams, as well as between process and utilities.

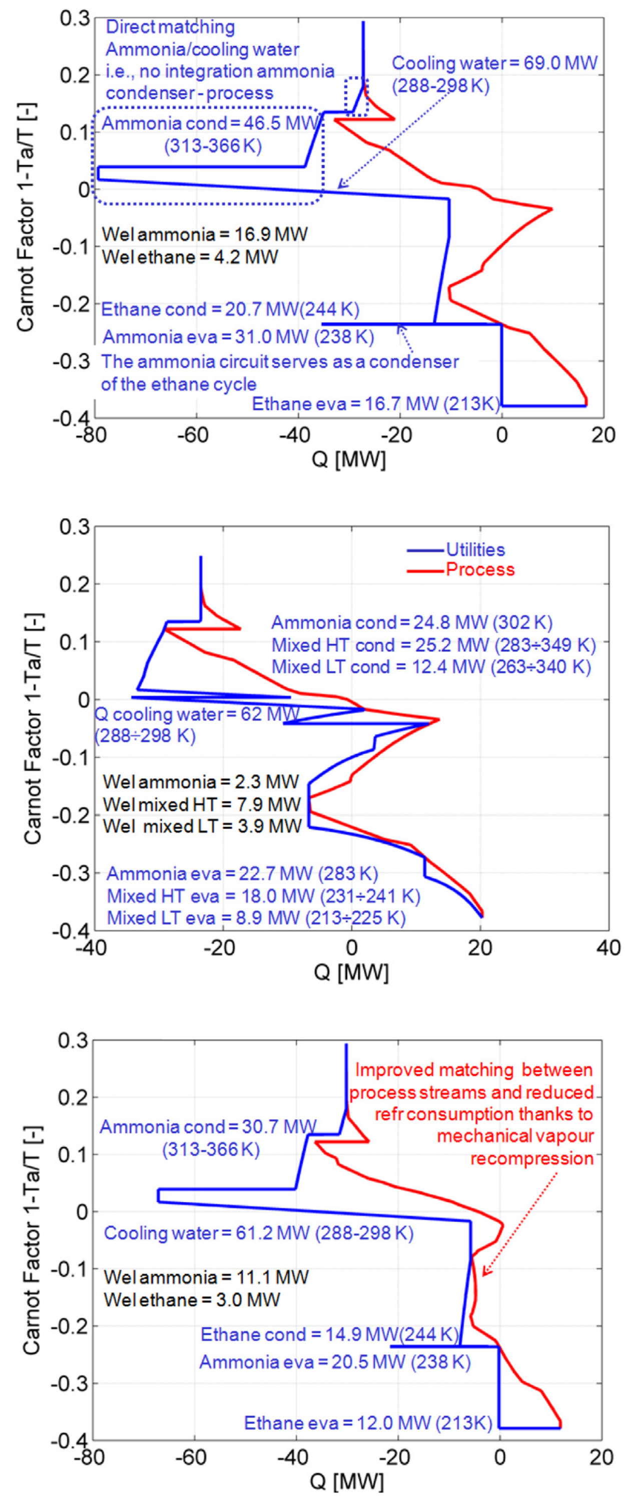

Fig. 12. Left: EGCC of Scheme A with two-level refrigeration cycle. Center: EGCC of Scheme A with mixed refrigerant. Right: EGCC of Scheme B with two-level refrigeration cycle.

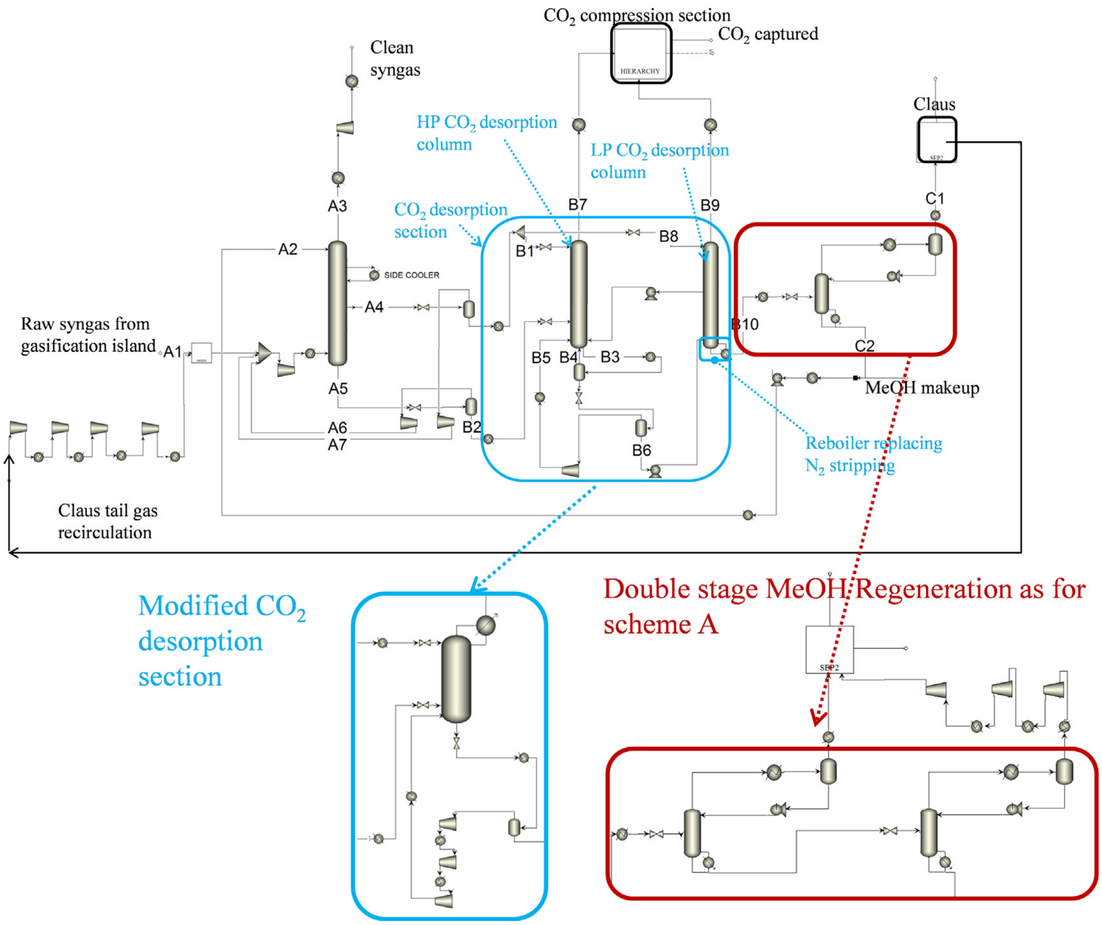

Fig. 13. Process flowsheet of scheme B, showing the details of the modified desorber.

5.2. Heat Integration results and novel schemes

First, we computed the SEEC of the Reference Rectisol® scheme integrated with the two-level refrigeration cycle performing steps 1–4 of the procedure described in the previous subsection. Main results are reported in Table 6, while the corresponding EGCCs are plotted in Fig. 10.

It is important to note that the main irreversibility sources are the usage of steam at 384 K for regenerating the methanol, and the heat transfer irreversibility in the temperature range between 213 and 300 K. This observation spurred us to carry out two main process modifications:

(i) Split the regeneration section in two columns as reported in Fig. 11 so as to reduce the energy consumption and the temperature level of the reboiler; the first regenerator remains at 1.2 bar, whereas the second operates sub-atmospheric at 0.7 bar. In this way, it is also possible to use some hot streams of the process (e.g., the streams exiting the process compressors) to supply a fraction of the reboiler heat duty. Hereafter this process scheme is called “Scheme A”.

(ii) Use the mixed-refrigerant cycle whose evaporator and condenser follow better the T–Q profile of the process in order to improve the Heat Integration in the low-temperature region.

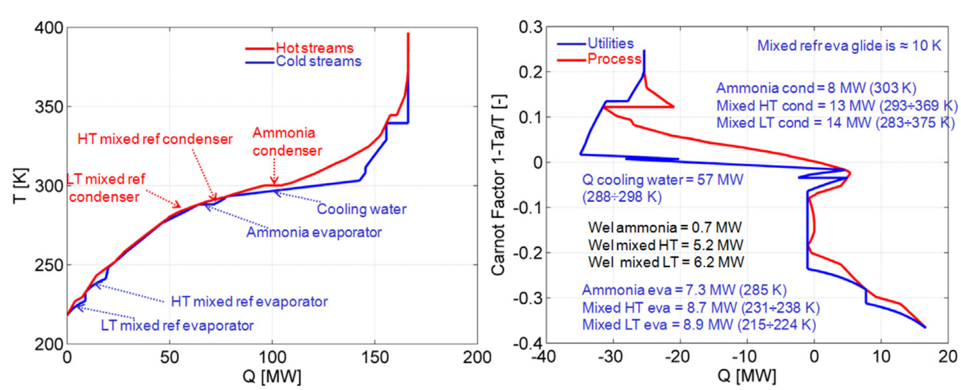

Fig. 14. CC and EGCC of Scheme B featuring the mixed refrigerant cycle.

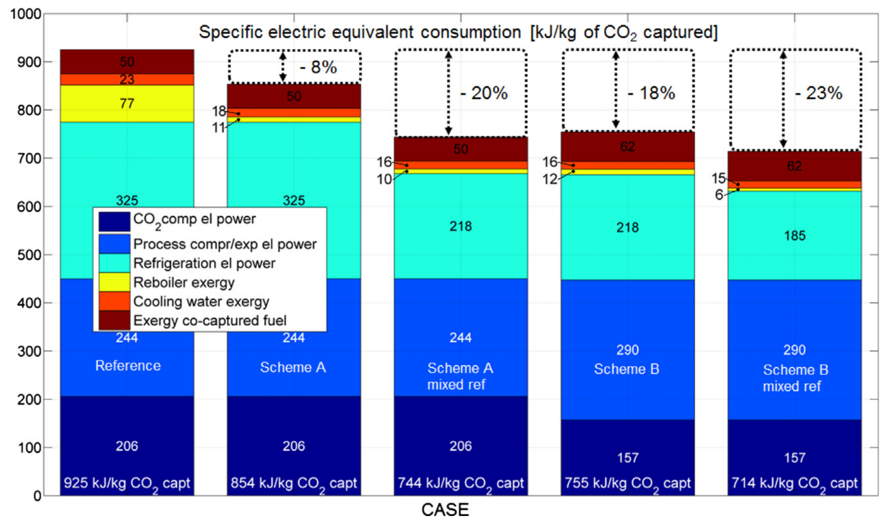

Fig. 15. Performance summary and breakdown analysis of the specific consumption for each case.

Hence, we repeated the process simulations, Heat Integration and SEEC calculation for the following two modifications:

- Scheme A with a state-of-the-art two-level refrigeration cycle
- Scheme A with mixed refrigeration cycle

Fig. 12, showing the EGCCs of the two improved cases, indicates that the reboiler modification of Scheme A appreciably reduces the heat transfer exergy penalty (i.e., the area between the red and blue curves), and that the mixed refrigerant cycle makes an even larger improvement. On the other hand, this refrigerator is more expensive and complex to operate and control than the two-level cycle.

For this reason, we found a simpler and more attractive way to reduce the refrigeration heat duty by looking at the internal Heat Integration of the process. We replaced the original two-column-based desorption section with a single-column desorber featuring a mechanical vapor recompression system which provides auto-refrigeration while vaporizing the CO_2 remained in the liquid methanol stream (see Fig. 13). In this arrangement, the desorption column is operated at a higher pressure (10 bar) so as to get a good compromise between the power consumption of the CO_2 compressor and that of the recycle compressors. The column is fed with the CO_2-loaded methanol (streams B1 and B8) which flashes releasing CO_2 and scrubs the gas flow to capture the vaporized H_2S. Since this scrubbing effect is not sufficient to meet the tight limit on the H_2S concentration of the CO_2 stream, a top condenser was added. It requires 4 MW of refrigeration power in the temperature range 232 ÷ 257 K. The H_2S-loaded methanol (stream B2 in Fig. 13) enters the column partly vaporized above the last stage, while stream B5 (richer in H_2S) coming from the mechanical vapor recompression system is fed at the last stage of the column. This layout allows the methanol of stream B1 to re-absorb most of the H_2S associated to streams B2 and B5. The liquid exiting the column is then adiabatically flashed to 2.2 bar and heated to provide refrigeration power (i.e., to have an auto-refrigeration effect) between 243 and 278 K, and therefore to reduce the power consumption of the refrigeration cycle. Hereafter the process configuration including the two-columns reboiler (Fig. 13) and the single-column CO_2 desorber is called "Scheme B".

Also for Scheme B, two Heat Integration options were evaluated, the first one with the two-level refrigeration cycle, and the second one with the mixed refrigerant cycle. The CC and EGCC of the option with the mixed refrigerant cycle are shown in Fig. 14. The main results and performance indexes are reported in Table 6 and Fig. 15. The internal auto-refrigeration reduces by about 33% the electric power of the refrigerator (−6.9 MW), saving 99 kJ/kg of CO_2 captured. It is worth noting that this modification reports an increase in the compression power of the process (+3 MW) caused by the mechanical vapor recompression but this increase is compensated by the decrease of the consumption of the CO_2 compressor which takes advantage of the higher pressure of the CO_2 desorption column. Indeed, in Scheme B the CO_2 desorption column operates at 10 bar while in the Reference case the HP and LP CO_2 desorbers work at 6 and 2.7 bar. This result, i.e., the advantage of operating the CO_2 desorbers at high pressures, appears to be reasonable for CCS. The maximum energy penalty reduction achievable by combining all of the proposed modifications (Scheme B with mixed refrigerant cycle) is 211 kJ/kg of CO_2 captured, corresponding to a decrease of 23% compared to the Reference case. In case of Scheme B with the less complex two-level refrigeration cycle, a reduction of 18% is reached.

It is also worth mentioning that most of the compression power required by the process derives from the raw syngas compressor (12.3 MW) whose consumption depends almost exclusively on the absorption pressure (kept constant throughout all the analysis).

6. Conclusions

This work investigates different configurations and Heat Integration options for Rectisol®-based processes for CCS. The analysis is focused on a Coal To Liquids facility whose main specifications are a high CO_2 capture level (98%) and the limits on the captured stream typically considered for EOR applications.

First a review of the Rectisol® schemes proposed by engineers and researchers is provided, focusing on the schemes relevant for CCS applications and their related issues. Then, the study provides updated information about the calibration of the PC-SAFT EOS suitable for the simulation of methanol absorption processes, showing that it is possible to predict the VLE bubble and dew point pressures with an average error lower than 7% for the methanol-CO_2/H_2S binary pairs, and lower than 2% for the H_2S-CO_2 pairs. The calibrated equation of state is used to simulate with Aspen Plus® a Reference Rectisol® scheme for CCS. Finally, the Heat Integration technique of Marechal and Kalitventzeff [42] together with the analysis of the Exergy Grand Composite Curves are applied to derive more efficient designs with optimized Heat Integration and utilities. The modifications introduced on the process side, i.e. staged regeneration and auto-refrigeration via mechanical vapor recompression, lead to a 18% reduction of the specific electric equivalent consumption compared to the Reference Case (755 against 925 kJ/kg of CO_2 captured), thanks to a decrease in the amount of steam bleeded for reboiling and in the external refrigeration duty.

A further 5% reduction, reaching a final specific consumption of 714 kJ/kg of CO_2 captured, could be reached by replacing the basic ammonia/ethane-cascade refrigerator with a three-level-mixed-refrigerant cycle.

Acknowledgements

The authors acknowledge Dr. Thomas Kreutz (Princeton University) for the useful suggestions and interesting discussion on the Rectisol® process, and Dr. Laurence Tock (EPFL) for introducing Osmose to Manuele Gatti, and providing useful support. The authors are grateful to Politecnico di Milano and LEAP (Laboratorio Energia Ambiente Piacenza) for funding the activity of Manuele Gatti, and to Ecole Polytechnique Fédérale de Lausanne-IPESE for hosting him during this research.

Nomenclature and symbols

ΔT_{MIN}	minimum approach temperature difference
T_a	ambient temperature
AGR	acid gas removal
CCS	carbon capture and storage
COP	coefficient of performance
CTL	coal to liquid fuels
EOR	enhanced oil recovery
EOS	equation of state
FT	fischer–tropsch
IGCC	integrated gasification combined cycle
LHV	lower heating value
MILP	mixed integer linear program
PC-SAFT	perturbed-chain statistical associating fluid theory equation of state
SEEC	specific electric equivalent consumption
SNG	substitute natural gas
VLE	vapor–liquid equilibrium
WGS	water gas shift

References

[1] D.A. Bell, B.F. Towler, M. Fan, Coal Gasification and its Applications, Elsevier, Amsterdam (The Netherlands), 2011.

[2] MIT, CCS Project Database, 2013, Available at sequestration.mit.edu, (Last consulted on 24/12/2013).

[3] USA DOE-NETL, Carbon Dioxide Enhanced Oil Recovery – Untapped Domestic Energy Supply and Long Term Carbon Storage Solution, 2010. Available at: www.netl.doe.gov/file%20library/research/oil-gas/CO2_EOR_Primer.pdf (Last consulted on 24/12/2013).

[4] IEA, World Energy Outlook, IEA, Paris Cedex 15 (France), 2013. Available at: www.worldenergyoutlook.org/ (Last consulted on 24/12/2013).

[5] G. Liu, E.D. Larson, R.H. Williams, T.G. Kreutz, X. Guo, Making Fischer–Tropsch fuels and electricity from coal and biomass: performance and cost analysis, Energy Fuels 25 (1) (2010) 415–437.

[6] T.G. Kreutz, E.D. Larson, G. Liu, R.H. Williams, Fischer-Tropsch fuels from coal and biomass, in: 25th Annual International Pittsburgh Coal Conference, vol. 29, 2008 September. No. 2.10), Pittsburgh (USA).

[7] C.A. Floudas, J.A. Elia, R.C. Baliban, Hybrid and single feedstock energy processes for liquid transportation fuels: a critical review, Comput. Chem. Eng. 41 (2012 June) 24–51.

[8] C. Higman, State of the gasification industry – the updated worldwide gasification database, in: Gasification Technologies Conference, Colorado Springs (USA), 2013 October. Available at: http://www.gasification.org/database1/GTC2013-Higman-Paper.pdf (Last consulted on 24/04/2014).

[9] USA DOE-NETL, Proposed Gasification Plant Databases (U.S. and Non-U.S. projects), 2013. Available at: www.netl.doe.gov/technologies/coalpower/gasification/worlddatabase/ (Last consulted on 24/12/2013).

[10] E. Martelli, T. Kreutz, M. Carbo, S. Consonni, D. Jansen, Shell coal IGCCS with carbon capture: conventional gas quench vs. innovative configurations, Appl. Energy 88 (11) (2011) 3978–3989.

[11] Herbert W., Kohrt H. U., Becker R., Danulat F., US Patent number 2,863,527, 1958.

[12] Ranke G., Weiss H., Separation of Gaseous Components From a Gaseous Mixture by Physical Scrubbing, US Patent number 4,324,567, 1982.

[13] A.L. Kohl, R. Nielsen, Gas Purification, Gulf Publishing, Houston (USA), 1997.

[14] A. De Klerk, Fischer–Tropsch Refining, Wiley-VCH Verlag & Co., Weinheim (Germany), 2011.

[15] AirLiquide-Lurgi, The Lurgi FBDBTM gasification island solutions to the challenges, in: Third World Petro Coal Congress, New Delhi (India), 2013 February. Available at: www.worldpetrocoal.com/html/presentation/Siddhartha_Mukherjee.pdf (Last consulted on 24/04/2014).

[16] T. Haberle, C. Geraghty, Keys to optimized and integrated poly-gen projects, in: Gasification Technologies Conference, San Francisco (USA), 2011 October. Available at: www.gasification.org/library (Last consulted on 24/04/2014).

[17] U. Koss, Rectisol expands its scope in China (Lurgi AG), in: Presented at the Gasification Technologies Conference 2006, Washington (USA), 2006. Available at: www.gasification.org/library (Last consulted on 24/04/2014).

[18] USA DOE-NETL, Quality Guidelines for Energy System Studies, in: CO_2 Impurity Design Parameters, 2013 August. DOE/NETL-341/011212 Draft Report USA.

[19] Ranke G., Weiss H., Scrubbing system yielding high concentration of hydrogen sulfide. US Patent number 4,430,316, 1984.

[20] G. Hochgesand, Rectisol and purisol, in: European and Japanese Chemical Industries Symposium, vol. 62, 1970 n.7.

[21] H. Weiss, Rectisol wash for purification of partial oxidation gases, Gas Sep. Purif. 2 (December) (1988).

[22] L. Sun, R. Smith, Rectisol wash process simulation and analysis, J. Clean. Prod. 39 (1) (2013) 321–328.

[23] E.-I. Koytsoumpa, K. Atsonios, K.D. Panopoulos, S. Karellas, E. Kakaras, J. Karl, Modelling and assessment of acid gas removal processes in coal-derived SNG production, Appl. Therm. Eng. (2014) (Article in press), http://dx.doi.org/10.1016/j.applthermaleng.2014.02.026.

[24] USA DOE, Practical Experience Gained During the First Twenty Years of Operation of the Great Plains Gasification Plant and Implications for Future Projects, 2006 (USA DOE Report).

[25] B. Munder, S. Grob, P.M. Fritz, Selection of wash systems for sour gas removal, in: Fourth International Freiberg Conference on IGCC & XtL Technologies, Freiberg (Germany), May, 2010. Available at: www.gasification-freiberg.org/PortalData/1/Resources/documents/paper/IFC_2010/14-1-Fritz-Munder.pdf (Last consulted on 24/04/2014).

[26] M. Kasper, Syngas Conditioning by Lurgi Rectisol, May 2009. Technical presentation from fifth IEA Task workshop 'Biomass Gasification Raw Gas Cleaning, Conditioning, and Conversion.', Karlsruhe (Germany).

[27] E.W. Lemmon, R.T. Jacobsen, S.G. Penoncello, D.G. Friend, Thermodynamic properties of air and mixtures of nitrogen, argon, and oxygen from 60 to 2000 K at pressures to 2000 MPa, J. Phys. Chem. Ref. Data 29 (3) (2000) 331.

[28] O. Kuntz, W. Wagner, The GERG-2008 wide-range equation of state for natural gases and other mixtures: an expansion of GERG-2004, J. Chem. Eng. Data 57 (11) (2012) 3032–3091.

[29] AspenTech. Aspen Plus® version 7.3, USA.

[30] J. Gross, G. Sadowski, Perturbed-chain SAFT: an equation of state based on a perturbation theory for chain molecules, Ind. Eng. Chem. Res. 40 (4) (2001) 1244–1260.

[31] N.I. Diamantonis, G.C. Boulougouris, E. Mansoor, D.M. Tsangaris, I.G. Economou, Evaluation of cubic, SAFT, and PC-SAFT equations of state for the vapor–liquid equilibrium modeling of CO2 mixtures with other gases, Ind. Eng. Chem. Res. 52 (10) (2013) 3933–3942.

[32] N.I. Diamantonis, I.G. Economou, Evaluation of statistical associating fluid theory (SAFT) and perturbed chain-SAFT equations of state for the calculation of thermodynamic derivative properties of fluids related to carbon capture and sequestration, Energy Fuels 25 (7) (2011) 3334–3343.

[33] R.W. Rousseau, J.N. Matange, J.K. Ferrell, Solubilities of carbon dioxide, hydrogen sulfide, and nitrogen mixtures in methanol, AIChE J. 27 (4) (1981) 605–613.

[34] A.D. Leu, J.J. Carroll, D.B. Robinson, The equilibrium phase properties of the methanol-hydrogen sulfide binary system, Fluid Phase Equilib. 72 (1992) 163–172.

[35] Gelbeim, PEP Review 2008-2 Acid Gas Removal (Review 2008-2), SRI Consulting, Menlo park (California) USA, 2008. Available at: http://www.ihs.com/products/chemical/technology/pep/reviews/index.aspx (Last consulted on 24/04/2014).

[36] NIST, M. Frenkel, R.D. Chirico, V. Diky, C. Muzny, E.W. Lemmon, X. Yan, Q. Dong, NIST ThermoData Engine. NIST Standard Reference Database 103b, Version, 5, 2008.

[37] Mathworks. MATLAB® R2012a.

[38] G.P. Van der Laan, Kinetics, Selectivity and Scale up of the Fischer-Tropsch Synthesis, PhD Thesis, University of Groningen, The Netherlands, 1999.

[39] Prelipceanu A., Kaballo H. P., Kerestecioglu U., Linde Rectisol® wash process. 2nd International Freiberg Conference on IGCC & XtL Technologies, Oral presentation (lecture 7.5), Freiberg (Germany) 8–12 May, 2007.

[40] A. Aspelund, D.O. Berstad, T. Gundersen, An extended pinch analysis and design procedure utilizing pressure based exergy for subambient cooling, Appl. Therm. Eng. 27 (16) (2007) 2633–2649.
[41] J. Klemes (Ed.), Handbook of Process Integration (PI): Minimisation of Energy and Water Use, Waste and Emissions, Elsevier, Amsterdam (The Netherlands), 2013. ISBN: 978-0-85709-593-0.
[42] F. Marechal, B. Kalitventzeff, Process integration – selection of the optimal utility system, Comput. Chem. Eng. 22 (1998) 149–156.
[43] M. Escobar, J.O. Trierweiler, Optimal heat exchanger network synthesis: a case study comparison, Appl. Therm. Eng. 51 (1–2) (March 2013) 801–826.
[44] A.I.A. Salama, Optimization techniques for heat exchanger networks using the minimum rule (MR), Appl. Therm. Eng. 45 (2012) 108–117.
[45] M. Gassner, F. Maréchal, Methodology for the optimal thermo-economic, multi-objective design of thermochemical fuel production from biomass, Comput. Chem. Eng. 33 (3) (2009) 769–781.
[46] A. Makhorin, GLPK (GNU Linear Programming Kit), Release 4.41, 2009.
[47] preprint of 2007 (authors of the first edition Linnhoff, B., Townsend, D. W., Boland, D., Hewitt, G. F., Thomas, B. E. A., Guy, A. R. and Marsland, R) I.C. Kemp, Pinch Analysis and Process Integration. A User Guide on Process Integration for Efficient Use of Energy, Elsevier, the Netherlands, Amsterdam, 2011.